Bergman cyclopolymerization kinetics of bis-*ortho*-diynylarenes to polynaphthalene networks. A comparison of calorimetric methods

H.V. Shah[a], D.A. Babb[b], D.W. Smith Jr.[a],*

[a]*Department of Chemistry, Clemson University, Clemson, SC 29634, USA*
[b]*The Dow Chemical Company, Freeport, TX 77541, USA*

Abstract

Bis-*ortho*-diynylarene (BODA) monomers undergo radical mediated Bergman-type cycloaddition polymerization to yield polynaphthalene networks. This report describes the use of conventional and modulated temperature differential scanning calorimetry to compute the cure kinetic parameters of BODA monomers with different spacer groups. Three different kinetic methods employed here utilize non-isothermal dynamic thermal profiles to estimate activation energies ($E_a = 28.7$–33.5 kcal/mol [120–140 kJ/mol]) and the first order rate constants ($k \sim 10^{-5}$ s^{-1} at 210°C) of polymerization. The results obtained from these methods show surprisingly good mutual agreement and also reveal that varying the spacer group has marginal effect on the cure kinetics. It has also been shown that the reaction kinetic information obtained from the dynamic methods must be corrected, when applied under isothermal conditions, to account for sample vitrification. The correction factor has been estimated using modulated temperature differential scanning calorimetry which is capable of monitoring the sample heat capacity in real time. © 2000 Elsevier Science Ltd. All rights reserved.

Keywords: Bis-*ortho*-diynylarenes; Differential scanning calorimetry; Bergman cyclopolymerization kinetics

1. Introduction

The thermal cyclo-rearrangement of aromatic 1,2-diynes to 1,4-dehydroaromatic or naphthalene diradicals has received much attention since the first accounts by Bergman [1] nearly three decades ago (Scheme 1). Although the overwhelming impetus for enediyne research has been due to their use as biologically active antitumor agents [2], more recent reports have focused on the potential of the Bergman cyclization to prepare high performance linear aromatic polymers [3–5]. In the absence of radical termination reactions, polymerization is favored in an overall step growth addition type fashion (Scheme 1).

Linear polyarlyenes prepared by Bergman cyclopolymerization, however, suffer from the processability/performance trade-off issues which commonly plague high performance materials in general. To address this problem, we have designed bis-*ortho*-diynylarene (BODA) monomers containing two sets of aryldiynes per molecule [6]. A branching architecture in reactive intermediate oligomers imparts excellent solution and melt processability prior to thermoset cure. Phenyl substituted BODA monomers yield highly cross-linked polynaphthalene networks which exhibit high thermal stability (<1.5% wt.loss/h at 450°C) and undetectable glass transitions by calorimetry or thermomechanical analysis below 400°C. Monomers are prepared in high yield from common bisphenols thereby providing tremendous synthetic versatility and the opportunity to develop wide array of novel polyarylene thermosets by varying the aromatic spacer group, **X** (Scheme 2).

Although originally targeted for high temperature interlayer dielectric coatings in integrated circuits [6], BODA networks possess other interesting properties suitable for potential applications such as an active light emitting layer [7,8] in organic polymer based light emitting diodes (LED), matrix or carbon-carbon composites, and as micromolded precursors to electrically conducting high-carbon glasses for microelectromechanical systems (MEMS) [9,10].

Grissom [11,12], and more recently Russell [13] have detailed the kinetic analysis for the Bergman cyclization of substituted aromatic diynes by trapping the diradicals formed. Earlier work by Keller [5] and Grubs [14] described the use of calorimetry to study the thermolysis of Bergman cyclopolymerization. Our primary aim of the current work is to gain better understanding of the cure chemistry of tetrafunctional BODA monomers and intermediate resins

* Corresponding author. Tel.: +1-864-656-5020; fax: +1-864-656-6613.
E-mail address: dwsmith@clemson.edu (D.W. Smith Jr.).
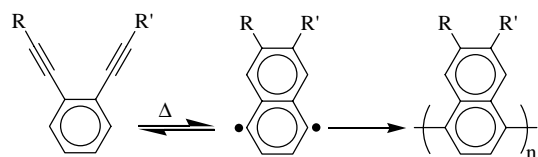
Scheme 1.

and to recognize the influence of the spacer (**X**) on the polymerization rate and cure conditions by comparing several calorimetric kinetics techniques. Four different BODA monomers have been chosen for this study as shown in Scheme 2.

Since the thermoset chemistry involves transformation of reactive oligonaphthalene melts to ultra high molecular weight solids, the state of the system is dependent on the temperature (T) and the chemical conversion (α); both of which can be easily monitored using differential scanning calorimetery (DSC). Here, we have used a conventional DSC to determine the reaction kinetics using three dynamic kinetic analysis techniques viz. nth order kinetics, ASTM E-698 thermal stability protocol [15], and Model-free kinetics [16].

Knowledge of kinetic parameters allows prediction of conversion vs. time for specific isothermal temperatures, which is extremely important from a practical processing standpoint. However, when a thermosetting material is cured isothermally at a temperature substantially below the glass transition temperature (T_g) of the fully cured network, the T_g of the growing network gradually approaches the cure temperature until the material vitrifies ($T_g = T_{cure}$) [17,18]. Near vitrification, the kinetics of

curing are often complex due to restricted molecular mobility and inter-molecular diffusion. The actual reaction rate near vitrification is substantially lower than theory predicts [17,19]. The decrease in the rate of reaction is coupled to restricted molecular mobility, which in turn is associated with the reduction in heat capacity. Here, we have also used the real-time heat capacity measurement capability of a modulated temperature differential scanning calorimeter (MTDSC) to better describe the isothermal kinetics of BODA resins [19].

2. Experimental

The synthesis and purification of BODA monomers (98 + %) and their polymerization details are described elsewhere [6–8]. A Mettler-Toledo DSC820 was used for conventional DSC scans and the MTDSC measurements were performed in a TA Instruments 2920 DSC equipped with a liquid nitrogen cooling accessory. Temperature and enthalpy calibrations were performed using indium on both systems. The heat capacity on MTDSC was calibrated using a 25 mg sapphire standard. About 8–10 mg of monomer sample were used for each experiment. The samples were sealed in aluminum hermetic pans with a pinhole and nitrogen was used as the purge gas. The samples were equilibrated in the purge gas for about 15 min prior to each run. For isothermal kinetic studies, the temperature of the cell was raised to the desired value before introducing the sample and the reference pans and data collection was initiated after stabilization of the sample temperature and heat flow. The sample and reference pans were matched
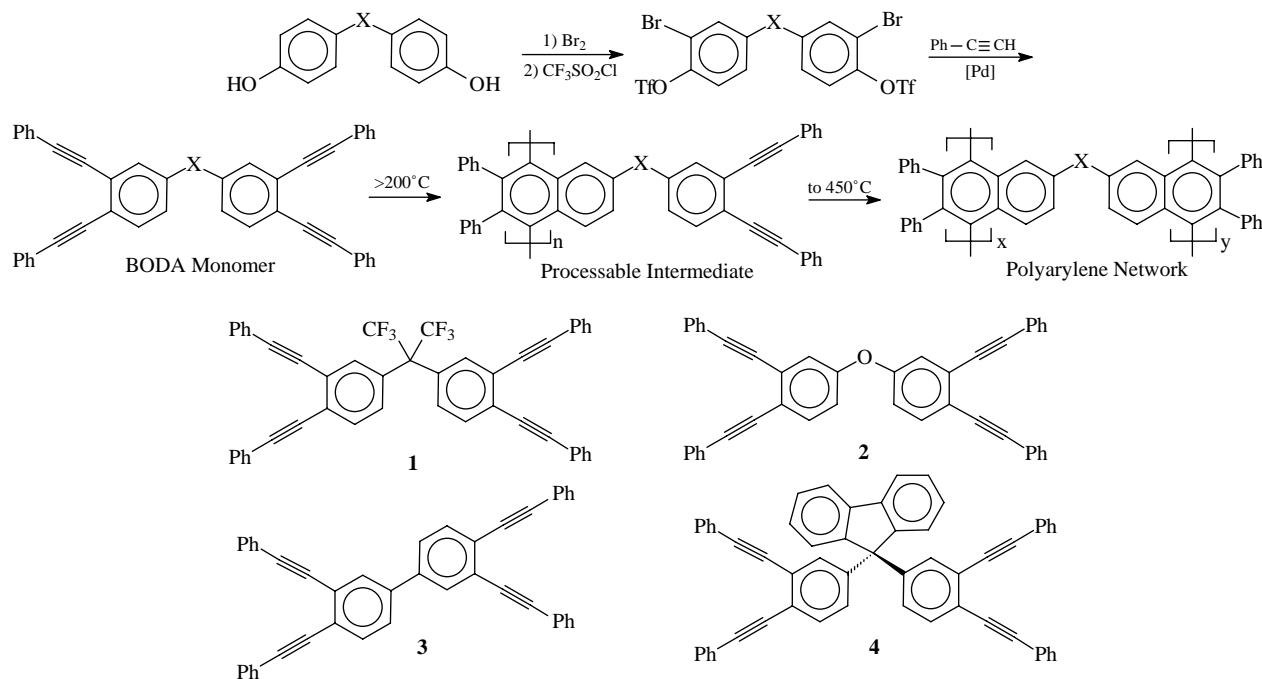
Scheme 2.

accurately to ±0.1 mg for isothermal heat capacity measurements and quasi-isothermal heating profiles were applied with a sinusoidal modulation amplitude of 0.5°C and a 60 s period. A sigmoidal baseline was used for all kinetic analyses to account for the shift in baseline due to change in the specific heat capacity of the resins.

3. Non-isothermal kinetic theory

3.1. Nth order kinetics

This approach was originally described by Borchardt et al. [20] and subsequently refined for solids by other researchers [21]. It permits the calculation of activation energy (E_a), pre-exponential factor (Z), reaction order (n), and rate constant (k) from a single DSC scan.

A reaction that follows nth order kinetics will obey the following general rate equation which, when combined with the Arrhenius temperature dependence of the rate constant, may be written as follows:

$$\frac{d\alpha}{dt} = Z \exp\left(-\frac{E_a}{RT}\right)(1 - \alpha)^n \qquad (1)$$

To obtain $d\alpha/dt$ and α in Eq. (1), the following relations are used:

$$\frac{d\alpha}{dt} = \frac{H}{A_{tot}}; \qquad \alpha = \frac{A_{par}}{A_{tot}} \qquad (2)$$

Where, H is the DSC signal deviation from baseline, A_{par} is the partial peak area and A_{tot} total peak area.

Usually several values of T, $d\alpha/dt$ and α in the range of investigation are obtained from one dynamic DSC peak to calculate Z, E_a and n by the method of least squares.

3.2. ASTM E-698 thermal stability

This kinetic approach is based on the variable program rate method of Ozawa [22] which requires three or more experiments at different heating rates. This approach is valid only for reactions following first order kinetics. For $n = 1$, Eq. (1) can be rearranged as follows:

$$\beta \frac{d\alpha}{dT} = Z \exp\left(-\frac{E_a}{RT}\right)(1 - \alpha) \qquad (3)$$

where, $\beta = dT/dt$ is the heating rate

Assuming that the extent of the reaction at the peak exotherm, α_p, is a constant and independent of heating rate, a plot of natural logarithm of the heating rate versus the peak temperature provides the information necessary to calculate E_a, Z and k. Refinements of the approximated activation energy are attained by reiterations using a fourth degree polynomial.

3.3. Model-free kinetics

The model-free kinetics is based on the theory proposed

by Vyazovkin [16]. Here, a more generalized form of rate equation is used as shown below:

$$\frac{d\alpha}{dt} = Z \exp\left(-\frac{E_a}{RT}\right) f(\alpha) \qquad (4)$$

The above equation may be integrated as follows:

$$\int_0^\alpha \frac{1}{f(\alpha)} d\alpha = g(\alpha) = \frac{Z}{\beta} \int_{T^0}^T \exp\left(-\frac{E_a}{RT}\right) dT$$

Since $E/RT \gg 1$, the temperature integral can be approximated as follows:

$$\int_{T^0}^T \exp\left(-\frac{E_a}{RT}\right) dT \approx \frac{R}{E} T^2 \exp\left(-\frac{E_a}{RT}\right)$$

Substituting the above temperature integral, rearranging and taking natural logarithm gives:

$$\ln \frac{\beta}{T\alpha^2} = \ln\left[\frac{RZ}{E\alpha g(\alpha)}\right] - \frac{E\alpha}{RT\alpha} \qquad (5)$$

The method requires three or more DSC scans at different heating rates from which conversion (α) versus temperature (T) plots are generated. According to Eq. (5), a plot of $\ln(\beta/T^2)$ versus $1/T$ for each conversion should be a straight line with the slope $-E_a/R$. Thus, the activation energy is obtained as a function of conversion.

Since the function $f(\alpha)$ is not solved for the evaluation, the theory is essentially model-free. This approach, thus, differs from the previous two in that it does not rely on "force-fitting" of experimental data to different reaction models. Therefore, the model-free approach permits more accurate kinetic and mechanistic interpretations especially for complex reactions, which cannot be described fully using a single mathematical model. It also allows for simulation of DSC curve for any heating rate and any sample size.

4. Isothermal kinetic theory

As mentioned earlier, prediction of isothermal kinetics during the final stages of cure require measurement of heat capacity due to vitrification and drastic reduction in reactive group mobility. A correction factor (CF) has been proposed to correct the kinetic rate equation for vitrification as shown below [19]:

$$\left(\frac{d\alpha}{dt}\right)_{EXP} = \left(\frac{d\alpha}{dt}\right)_{KIN} (CF) \qquad (6)$$

Where, $(d\alpha/dt)_{EXP}$ is the experimentally observed rate of conversion and $(d\alpha/dt)_{KIN}$ is the kinetically projected rate of conversion in the absence of any mobility and diffusion restrictions. The correction factor CF can be calculated directly from change in the heat capacity of the material as shown below:

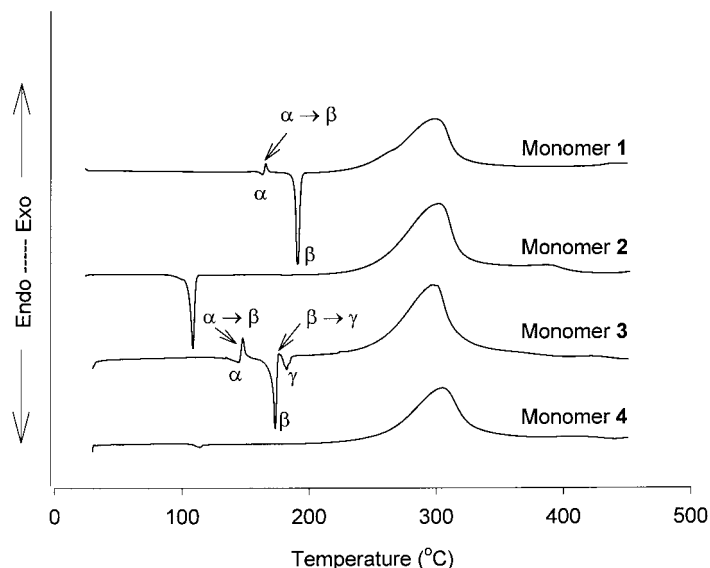$$CF = \frac{C_p - C_{p_g}}{C_{p_\ell} - C_{p_g}} \qquad (7)$$

Fig. 1. DSC scans of BODA monomers from 35 to 450°C at a heating rate of 5°C/min.

where, C_p is the heat capacity at a specific reaction time; C_{p_g} the heat capacity of the polymer in the glassy state after vitrification; and C_{p_ℓ} is the capacity of the polymer in the fluid state before vitrification.

Thus a plot of CF versus reaction time can be generated and a more accurate isothermal reaction rate can be predicted.

5. Results and discussion

5.1. Temperature and heat-flow analysis

Fig. 1 shows the DSC scans of the BODA monomers **1-4** from 25 to 450°C at a heating rate of 5°C/min. It can be observed that monomers **1** and **3** are polymorphic with the former showing at least two crystalline forms and the latter exhibiting three different polymorphs. Upon melting, the α form immediately recrystallizes to a more stable β form in both monomers. However, in case of monomer **3** the $\beta \rightarrow \gamma$ recrystallization is not readily observed. The melt endotherm of monomer **2** exhibits a small shoulder most likely due to the presence of another polymorph whose melting point is too close to the primary polymorph to be resolved by the DSC. It is also interesting to note that monomer **4** exhibits a weak endotherm indicative of either poor crystallization or extensive polymorphism.

The cure onset temperatures of **1–4**, measured as the point of intersection of the extrapolated baseline and the initial steep portion of the curve, are 227, 231, 232, and 228°C, respectively, and the corresponding peak exotherm temperatures are 299, 302, 299 and 305°C (refer to Table 1). The heat of polymerization values of **1–4** were found to be 26.5, 24.8, 26.8 and 25.0 kcal/mol alkyne, respectively. For comparison, 1,2-di(phenylethynyl)benzene, known to undergo Bergman cyclization to give linear polynaphthalenes, gave a DSC measured exotherm value of 29.5 kcal/mol alkyne [5,14].

The fact that the heat of polymerization of BODA compounds is less than the enthalpy associated with linear Bergman cyclizations suggests that BODA monomers may not experience complete conversion under these conditions due to their rapid vitrification and ultimate high cross link density. It was also observed that the heat-flow profiles and heat of polymerization of BODA monomers were consistent with other phenyl substituted aryldiynes that polymerize to networks [5].

5.2. Non-isothermal kinetic analysis

For determination of the kinetic parameters, polymerization of BODA monomers **1–3** was carried out in the DSC at three different heating rates of 5, 10 and 20°C/min. Fig. 2

Table 1
Temperature and heat flow data for BODA monomers by DSC

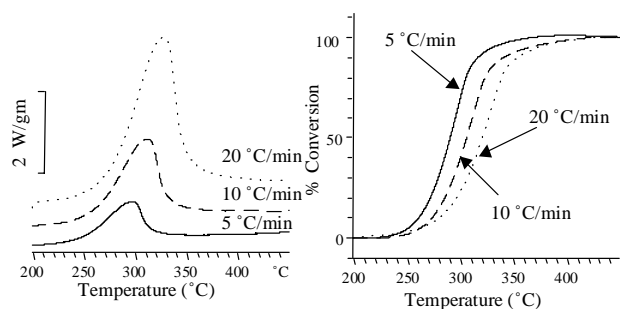| Monomer	Melting (°C)	Cure onset (°C)	Cure max (°C)	Enthalpy (kcal/mol alkyne)
1	$\alpha = 163$; $\beta = 190$	227	299	26.5
2	$\alpha = 108$	231	302	24.8
3	$\alpha = 144$; $\beta = 173$; $\gamma = 182$	232	299	26.8
4	$\alpha = 114$	228	305	25.0

Fig. 2. DSC scans and conversion plots for monomer **1** obtained at heating rates of 5 (solid line), 10 (dashed line), and 20 (dotted line)°C/min.

shows the peak of interest for the monomer **1**, as an example. In each case, as the heating rate is increased, the exothermic peak shifts towards higher temperature. This effect of heating rate on the reaction dynamics can be more clearly observed in the corresponding conversion plots. Complete conversion converges for each monomer above 400°C, independent of heating rate. The kinetic parameters for each monomer were calculated from the dynamic DSC scans such as those shown in Fig. 2 using the previously described non-isothermal methods. The results are presented in Table 2.

Since only one dynamic DSC scan is required for estimation of kinetic parameters by the nth order technique, a set of three values were obtained for each monomer. On comparison, very good consistency of activation energies and pre-exponential factors were observed for each monomer, illustrating the reproducible nature of BODA polymerization under different thermal conditions.

The ASTM E-698 approach takes into account only the peak height and peak temperature as the heating rate is varied. Therefore, this method is considered "a quick and dirty" analysis tool when simplicity and speed are preferred over accuracy. However, it was surprising to find very good mutual agreement between the nth order and ASTM E-698 approaches.

The Model-free kinetic approach has been developed very recently and hence has not been widely used [16]. This kinetic approach calculates the activation energy as a function of conversion as shown in Fig. 3. Constant activation energies, as observed in Fig. 3, for each monomer throughout the entire reaction is indicative of the reaction following simple nth order kinetics without occurrence of any autocatalytic events. The steep slopes observed in these plots at the start and the end of the reaction are due to large mathematical errors. The average value for each monomer from the plots in Fig. 3 is tabulated along with the kinetic parameters from other techniques where once again, the average activation energies obtained using this method are in good agreement with the corresponding values obtained from nth order and ASTM methods.

Slight variations are observed in the activation energies for BODA monomers **1**–**3**, with the energy for **1** being lowest and that for **3** being highest. However, this change in activation energy is also accompanied by a compensating change in the pre-exponential factor Z thereby maintaining the rate constant values within same order of magnitude for the temperature range of interest. For example, at 210°C the reaction rate constants are 4.1×10^{-5}, 2.8×10^{-5} and 3.1×10^{-5} s^{-1} for the monomers **1**, **2** and **3**, respectively.

It is known that the steric nature of the acetylene terminus—and thus the planarity of the cyclic transition state—and electronic effects of the substituents influence the rate of diradical formation in Bergman cyclization [11–13]. However, it appears that steric factors by far outweigh the electronic effects on the rate of cyclization of phenyl substituted monomers **1**–**3**. Since variation of the spacer group (**X**) only contributes to the electronic effects, we conclude that the rate of polymerization is not measurably influenced for the BODA monomers studied here.

5.3. Isothermal kinetic analysis

The final stages of curing for most thermoset resins under isothermal conditions are affected by reduced mobility and diffusion of reactive terminal groups, which can be identified by the vitrification of the growing network. Hence, kinetic analyses based on previously described dynamic methods when applied to isothermal conditions often lead to erroneous conclusions. In conventional DSC, vitrification may be observed indirectly as a decrease in the rate of

Table 2

Kinetic data and method comparison for BODA monomers **1-3**

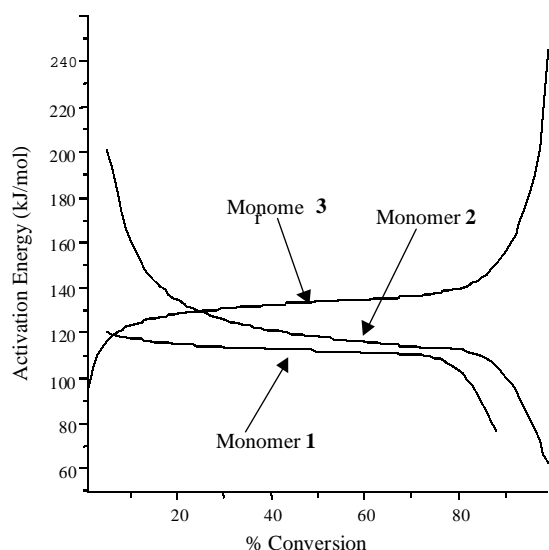| Monomer	Heating rate °C/min	nth Order			ASTM E-698	Model-free
		E_a (kcal/mol)	$\ln Z$ (s^{-1})	n		
1	5	31.1±0.2	21.9±0.1	0.9	$E_a = 29.7 \pm 0.8$ kcal/mol	$E_a = 28.7 \pm 1.3$ kcal/mol
	10	29.7±0.3	20.7±0.2	0.8		
	20	29.7±0.3	20.8±0.2	0.8	$\ln Z = 20.6 \pm 0.3$	
2	5	31.3±0.3	22.1±0.2	0.8	$E_a = 30.6 \pm 0.6$ kcal/mol	$E_a = 29.9 \pm 3.1$ kcal/molc
	10	31.3±0.3	21.9±0.3	0.8		
	20	31.3±0.4	21.9±0.3	0.8	$\ln Z = 21.4 \pm 0.4$	
3	5	33.3±0.1	24.3±0.1	0.8	$E_a = 32.5 \pm 0.5$ kcal/mol	$E_a = 31.1 \pm 3.2$ kcal/mol
	10	33.3±0.2	24.3±0.2	0.9		
	20	32.8±0.2	23.9±0.1	0.8	$\ln Z = 23.5 \pm 0.3$	

Fig. 3. Activation energy (E_a) as a function of conversion for monomers **1**–**3** as predicted by Model-Free kinetics.

reaction by performing a number of isothermal experiments. However, this technique is quite time consuming and tedious. Since heat flow and heat capacity can be measured simultaneously in a single scan, MTDSC offers greater insight into vitrification behavior of a thermosetting system [19].

BODA monomers **1** and **2** were polymerized quasi-isothermally at three different temperatures and their heat capacity (C_p) measured as a function of time using MTDSC. The observed C_p data for each monomer was converted into plots of CF versus time (Fig. 4) using equations described in the earlier section. Table 3 shows the vitrification time (t_{vit}) for each monomer at each isothermal temperature. The vitrification time was considered to be the time at half of the heat capacity change as suggested by Assche et al. [19]. This was

determined from the half-height of the difference between two extrapolated tangents to the baseline before and after vitrification.

As observed in Fig. 4, the CF is close to unity at the start of the reaction and drops marginally as the curing proceeds due to a corresponding drop in C_p for monomers **1** and **2**. When the material reaches a state of vitrification, CF drops drastically and quickly reaches zero signifying a premature end of curing. At all temperatures, monomer **1** was found to vitrify at a quicker rate than monomer **2** due to lower activation energy and higher rate constant of **1** compared to **2** as shown in the previous section. Since the rate constant bears an Arrhenius exponential relationship to the activation energy, the widening gap between the vitrification of monomers **1** and **2** with the increasing temperature is clearly evident from the logarithmic time scale of Fig. 4 and Table 3.

The implications of the above results are shown, for example, in the form of several plots in Fig. 5 for the case of monomer **2**. As predicted by dynamic DSC analyses, monomer **2** will take more than 30 h to achieve 100% conversion at 210°C. The same figure also shows the expected rate of reaction ($d\alpha/dt$) in the absence of mobility restrictions. However, the actual reaction rate (as calculated from specific-heat data using Eq. (6)) deviates significantly from the expected rate and decreases to zero much faster than the predicted rate. As a result, the ultimate conversion is limited to less than 80% at 210°C due to sample vitrification. Further cross-linking may be achieved only by increasing the conformational entropy of the growing chains, and thus the mobility of the reactive groups for further propagation.

6. Conclusions

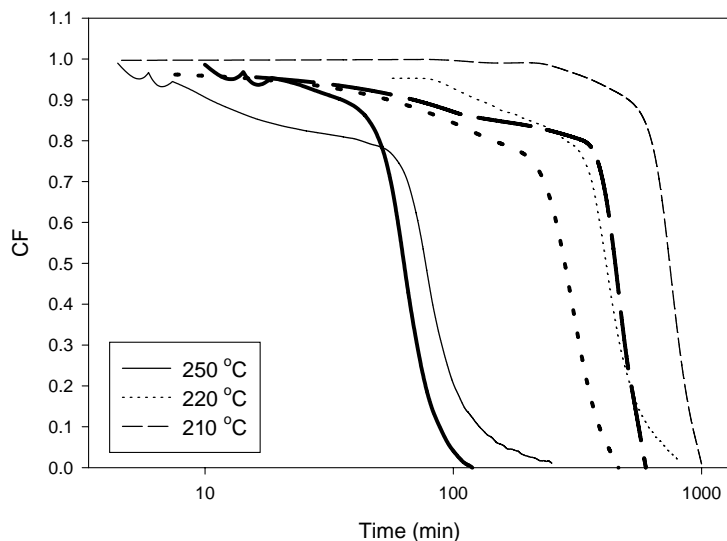Thermal cycloaddition polymerization kinetics for

Fig. 4. Plot of CF as a function of cure time for monomers **1** (thick line) and **2** (thin line) at 210, 220 and 250°C.

Table 3
Estimated vitrification times for monomers **1** and **2**

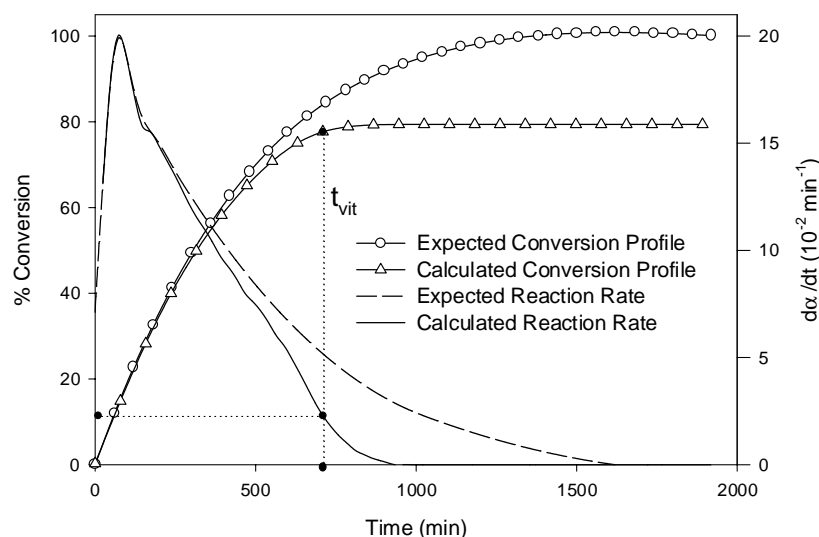| Isothermal temperature (°C)	Monomer **1** t_{vit} (min)	Monomer **2** t_{vit} (min)
210	739.4	448.1
220	427.2	303.3
250	77.8	64.7

Fig. 5. First order reaction rate and % conversion as a function of reaction time for the cure of BODA monomer **2** at 210°C.

BODA monomers has been investigated exclusively using DSC. The evaluation of kinetic parameters by three dynamic methods shows very good mutual agreement. The kinetic information obtained from the dynamic methods has been successfully applied towards isothermal cure experiments by deriving a correction factor which serves as the ratio of the observed rate of reaction to the rate predicted by chemical kinetics modeling (in the absence of diffusion control and vitrification). Thus, we have shown that by combining several experimental and data analysis techniques on a single analytical platform, considerable information and understanding can be obtained on curing kinetics of BODA monomers. These results will further serve a variety of fabrication processes currently under development for these new materials.

References

[1] Bergman RG. Acc Chem Res 1973;6:25.
[2] Nicolau KC, Dai WM. Angew Chem, Int Ed Engl 1991;30:1387.
[3] John JA, Tour JM. J Am Chem Soc 1994;116:5011.
[4] John JA, Tour JM. Tetrahedron 1997;53:15515.
[5] Sastri SB, Keller TM, Jones KM, Armistead JP. Macromolecules 1993;26:6171.
[6] Smith Jr DW, Babb DA, Snelgrove RV, Townsend PH, Martin SJ. J Am Chem Soc 1998;120:9079.
[7] Shah H, Babb DA, Smith Jr DW. Polym Mater Sci Engng (Am Chem Soc Proc) 1999;80:199.
[8] Shah H, Smith, DW Jr. In preparation.
[9] Shah H, Brittain ST, Huang Q, Hwu S-J, Whitesides GM, Smith Jr. DW. Polym Mater Sci Engng (Am Chem Soc Proc) 1999;81:23.
[10] Shah H, Brittain ST, Huang Q, Hwu S-J, Whitesides GM, Smith Jr. DW. Chem Mater 1999;11:2623.
[11] Grissom JW, Calkins TL, McMillen HA, Jiang Y. J Org Chem 1994;59:5833.
[12] Grissom JW, Calkins TL. J Org Chem 1993;58:5422.
[13] Kim C, Russell KC. J Org Chem 1998;63:8229.
[14] Grubbs RH, Kratz D. Chem Ber 1993;126:149.
[15] Standard Test Method for Arrhenius Kinetic Constants for Thermally

Unstable Materials (ANSI/ASTM E698-79) ASTM: Philadelphia, PA.

[16] Vyazovkin S, Goryachko V. Thermochim Acta 1992;194:221.

[17] Enns JB, Gillham JK. J Appl Polym Sci 1983;28:2567.

[18] Gillham JK. Encyclopedia of polymer science and engineering, 4. New York: Wiley, 1986. pp. 519–24.

[19] Assche GV, Hemelrijck AV, Rahier H, Mele BV. Thermochim Acta 1995;268:121.

[20] Borchardt HJ, Daniels F. J Am Chem Soc 1956;79:41.

[21] Swarin SJ, Wims AM. Anal Calorimetry 1976;4:155.

[22] Ozawa TJ. Thermal Anal 1970;2:301.